Title page

Title:

ZSM-5 ZEOLITES PERFORMANCE ASSESSMENT IN CATALYTIC PYROLYSIS OF PVC-CONTAINING REAL WEEE PLASTIC WASTES

Author names and affiliations:

Alessia Marino[a], Alfredo Aloise[a,b], Hector Hernando[c], Javier Fermoso[c], Daniela Cozza[a], Emanuele Giglio[a], Massimo Migliori[a], Patricia Pizarro[c,d], Girolamo Giordano[a], David P. Serrano[c,d,*]

[a]*CECaSP Lab University of Calabria, Via P. Bucci, I87036 Rende, (Italy).*

[b]*Department of Physical and Chemical Sciences, University of L'Aquila, Via Vetoio (COPPITO 1-2), 67100 L'Aquila (Italy).*

[c]*IMDEA Energy Institute, Avda Ramón de la Sagra, nº 3, E28935, Móstoles, Madrid (Spain).*

[d]*ESCET, Universidad Rey Juan Carlos, C/ Tulipán s/n, E28933, Móstoles, Madrid (Spain).*

Corresponding author*:

Tel.: +34 917371120; fax: +34 917371140. *E-mail address*: david.serrano@imdea.org (D.P. Serrano). Thermochemical Processes Unit, IMDEA Energy Institute, 28935, Móstoles, Madrid, Spain.

Abstract

Catalytic pyrolysis of plastic wastes is a promising way for their conversion into valuable products. By modulating the catalyst properties and operating conditions, it is possible to direct the product distribution to obtain oils that may be suitable both as fuels and as chemicals. However, the efficient and safe removal of the halogens, often contained in plastic wastes, remains as a great challenge. In this work, the catalytic behaviour of ZSM-5 zeolites in the pyrolysis of a real chlorinated plastic waste of the electric and electronic equipment sector (WEEE), consisting of PE with about 3.4% of PVC, was investigated. To that end, three zeolite samples with different acidity and accessibility were synthesized and assayed. A thermal pre-treatment was applied to the plastic waste at 350 ºC, which allowed a chlorine removal of 87 % from the WEEE feedstock. The pyrolysis tests were carried out in a downdraft fixed-bed stainless steel reactor, with a catalyst/feedstock ratio of 0.2, at temperatures of 600 ºC and 450 ºC in the thermal and catalytic zones, respectively, of the reaction system. In comparison with thermal pyrolysis, that mainly produced waxes, the product distribution changed considerably by contacting the pyrolysis vapours with ZSM-5 zeolites, leading to a strong enhancement in the yield of oil and gases. The largest yield of oil (about 60 wt.%), having a concentration of monoaromatics (mainly BTX) above 50 wt.%, was attained over the desilicated ZSM-5 sample. Regarding chlorine distribution, about 90 % was accumulated in the char fraction, probably captured by the inorganic components present in the raw WEEE waste. Coke was the second fraction in terms of Cl concentration, followed by wax and oil, whereas this halogen was almost not detected in the gases. The lowest concentration of Cl in the oil was attained with the desilicated zeolite, with a value below 90 ppm, which could facilitate the subsequent processing of this stream in refinery units.

Keywords: ZSM-5, pyrolysis, PVC-containing waste, WEEE, chlorine

1. Introduction

Within the current problem of the management of plastic wastes, those coming from electrical and electronic devices (e-wastes or WEEE) are becoming of increasingly concern. The consumption of this type of equipment has augmented significantly in recent years as they contribute to high standard of living and their large-scale production makes them affordable to a large part of society. However, they are usually short-lived products, hence, they quickly turn into wastes that are featured by a high heterogeneity and complexity, which add further challenges to the current waste management systems [1,2].

Current options for the management of plastic wastes include mechanical and chemical recycling, incineration and, as final option, disposal to landfills [2–4]. In fact, future schemes are being approved in many countries to reach zero-landfilling systems. Within chemical recycling, pyrolysis has been widely explored as an interesting alternative to produce fuels and/or other valuable chemicals from those plastics that cannot be mechanically recycled. Pyrolysis involve the thermal decomposition of plastics in absence of oxygen at temperatures in the range of 400-600 ºC, typically producing up to four fractions: gas, liquid (oil), wax and a carbonaceous solid (char). Optimising the reaction conditions, and in the presence of a catalyst (catalytic pyrolysis), the yield of oil can be maximised. The role of the catalyst is twofold: a) to boost the cracking reactions, allowing a higher depolymerisation of the feedstock and b) to drive the reaction system towards the formation of valuable compounds (e.g. monoaromatics) [3]. Among the catalysts investigated up to now, zeolites exhibit excellent performance due to their unique acidity and pore architecture [5,6]. In particular, ZSM-5 zeolite is recognised as one of the most remarkable catalysts due to is high cracking activity and relatively low coke generation [6,7].

Both porosity and acidity of ZSM-5 can be modified to modulate their activity, selectivity and resistance to deactivation. ZSM-5 zeolite possesses the MFI framework, having 10-membered rings and sinusoidal and straight intersecting channels with about 5.5 Å size. Such a micropore dimension is beneficial in terms of preventing deactivation by coke deposition and promoting the production of pyrolysis oils formed by light components. However, bulkier molecules typically present in plastic primary pyrolysis vapours cannot access to the active sites located in such micropores, hence, their conversion is limited to the external surface of the zeolite. In this regard, the development of hierarchical zeolites, with bimodal micro- and mesoporosity, has been a breakthrough in the field of polymers

cracking [5,8,9]. In particular, hierarchical ZSM-5 has revealed enhanced performance in the catalytic pyrolysis of polypropylene [8] and polyethylene [10–12]. On the other hand, the population and coordination of Al atoms in the MFI structure affect the strength and types of the zeolite acid centres (Lewis or Brønsted), having an important impact on the cracking activity [12,13].

One of the most commercially used polymers is PVC, whose high chlorine content (about 57 wt.%) represents a strong challenge for the viability of pyrolysis as valorisation route. Thus, oils produced by pyrolysis of PVC-containing plastics usually present a variety of chlorinated compounds, which make their use and further processing very difficult. Thermal decomposition of PVC occurs according to two characteristic stages: i) low-temperature dehydrochlorination of the polymer forming HCl and polyene chains and ii) high temperature decomposition of the latter producing gases, oil, wax and char. On the contrary, other plastics (PE, PP, PS) usually undergo thermal decomposition in a single-stage process [14,15].

A number of research works have been published about the pyrolysis of PVC-containing plastic mixtures [16–22], focusing their efforts on understanding the thermal degradation mechanism [16,18]. Besides, other articles have investigated the mass yields of the different products, concluding that the product distribution greatly depends on the operating conditions and, in particular, on the polymers mixture composition [15,21,22]. However, just a few works have studied the chlorine distribution among the pyrolysis products, showing that not all the Cl is removed in the form of HCl [19–21]. In this regard, Miskolczi et al. investigated the thermal pyrolysis of plastic waste mixtures of HDPE/PP/PS with PVC, concluding that the Cl content in the oil increased considerably with the PVC share (0.5-3 wt.%), reaching values over 2,000 ppm [21]. On the other hand, Bhaskar et al. [19] reported that chlorine distribution among the pyrolysis products varied strongly depending on the polymer mixture composition.

Therefore, pyrolysis of PVC-containing polymer mixtures produces oils with significant concentrations of organochloride compounds, hence, a dehydrochlorination step would be required before the oils can be commercially employed or processed in refinery units [23]. In this regard, Bhaskar et al. claimed the production of highly dechlorinated oils from a two-step thermal pyrolysis process of a simulated polymer mixture (PE/PP/PS) that included 10 wt.% PVC, whereas the chlorine concentration in the liquid fraction from a single-step pyrolysis was 390 ppm [20]. The impossibility to attain a chlorine-free oil

in single-step pyrolysis was attributed to the formation of chlorinated hydrocarbons by reaction between the released HCl and the olefinic hydrocarbons produced from PP/PS/PE. In a similar way, Uçar et al. achieved up to 98 % of dechlorination with a two-step thermal pre-treatment (30 min at 250 ºC, followed by 1 h at 350 ºC) of a simulated polymer mixture containing 5 wt.% PVC [23].

On the other hand, several materials, such as zeolitic catalysts [24–26], ordered mesoporous materials [26], clays [27] and natural limestone [28] have been employed for the catalytic conversion of PVC-containing plastic mixtures. Thus, Lin et al. [26] explored the effect of operating conditions and catalyst type, such as zeolites (HZSM-5, HUSY) or mesoporous materials (MCM-41), during the pyrolysis of a real post-consumer polymers mixture (PE/PP/PS) containing 1 wt.% PVC. However, little attention has been paid on the distribution of halogen compounds, typically present as additives (BFRs) or as intrinsic composition of the polymer (PVC) during the pyrolysis process. In one of these works, authors have evaluated the effect of ZSM-5 zeolite on the mass balances and Cl distribution during different configurations of catalytic pyrolysis using simulated PVC-containing plastic mixtures [25]. However, to the knowledge of the authors, there are no examples of catalytic pyrolysis of real plastic waste (containing PVC) employing zeolites as, in which, apart from the mass balances and oil composition, the evaluation of the Cl distribution has been investigated.

In this context, the current work investigates the catalytic pyrolysis of a real PVC-containing plastic waste (WEEE), with special focus on the chlorine distribution among the different products and, in particular, on its concentration in the oil fraction. Thereby, the feedstock has been firstly subjected to a dehalogenation thermal pre-treatment followed by a catalytic conversion step using a variety of ZSM-5 samples showing different acid sites concentration and accessibility. The results obtained here demonstrate that this combination is an efficient strategy for the production of an oil fraction with a significant yield and having a Cl content low enough to be finally processed in refinery units to produce both transport fuels and chemicals.

2. Materials and Methods

2.1. WEEE plastic sample

Waste plastic coming from the disposal of electric cables was supplied by R.Ed.El. srl, Italy. Prior to its utilisation, it was reduced in size and sieved to get particles in the range 0.5-1 mm.

2.2. Catalysts preparation

The syntheses of ZSM-5 zeolites were carried out using precipitated silica gel (SiO_2 100 %, Merck) as silica source, tetrapropylammonium bromide (TPABr 98%, Fluka) as structure directing agent, aluminium hydroxide ($Al(OH)_3$ 98%, Fluka) as Al source, sodium hydroxide (NaOH 97 %, Carlo Erba Reagenti) and ultrapure water. The gel composition was the following:

$$1\ SiO_2 - x\ Al_2O_3 - 0.08\ Na_2O - 0.08\ TPABr - 20\ H_2O \quad (1)$$

where the stoichiometric coefficient of aluminium (x) was varied to obtain Si/Al ratios equal to 11 and 25 (0.044 and 0.020, respectively).

The detailed procedure applied for the synthesis has been reported elsewhere [29,30]. The reactant mixture was stirred for 2 h at room temperature and then transferred to a Teflon-coated stainless-steel autoclave where it was heated up to 170 ºC in static conditions. The crystallisation time depended on the value of x (8 days for x = 0.044 and 4 days for x = 0.020). After cooling down the reactor, the solid was recovered by filtration, washed with distilled water and calcined in a tubular oven at 550 ºC for 8 h (heating rate of 5 ºC/min). The resulting zeolite, with Na^+ as counter-ion, was ion-exchanged twice with an aqueous solution of NH_4Cl (1 M, pH = 5.5) at 80 ºC for 2 h. The solid was then filtered and dried overnight (90 ºC). Finally, the zeolite in NH_4^+-form was thermally treated at 550 ºC for 8 h (5 ºC/min) to remove the ammonia and to obtain the final H^+-form. The synthesised samples were labelled as ZSM-5 (11) and ZSM-5 (25), according to their theoretical Si/Al ratio.

For the synthesis of the hierarchical ZSM-5, the H^+-form of ZSM-5 (25) was desilicated by using a 0.1 M solution of NaOH [31]. This treatment was carried out under stirring with a solution-to-solid ratio of 20 ml/g at 65 ºC for 60 minutes. At the end of the reaction, the suspension was filtered and the solid was ion-exchanged two consecutive times (1 M

NH_4Cl, 80 ºC, 2 h). Afterwards, the solid was calcined at 550 ºC for 8 h (heating rate = 5 ºC/min) to obtain the H^+-form of this material, named as ZSM-5 (25)_Des.

Prior to the catalytic tests, all the prepared zeolites were pelletised, grinded and sieved to obtain a particle size range of 180 – 250 μm.

2.3. Dechlorination treatments

Pre-treated WEEE samples were obtained via thermal dechlorination in a downdraft stainless-steel reactor (16 mm internal diameter and 400 mm length). About 5 g of plastic were loaded inside the reactor and then the system was purged with nitrogen to ensure an oxygen-free environment. Afterwards, the sample was heated up to 350 ºC with a heating rate of 10 ºC/min, then keeping the final temperature for 30 min. The flow of nitrogen was set as 50 ml/min during the whole procedure. The outgoing vapours were passed through a condensation system refrigerated at 0-4 ºC, consisting of a first flask to condense the organics and a series of two water-containing flasks (2 x 100 ml) for HCl solubilisation. The non-condensable gases were finally collected and quantified by means of a closed water-containing column, in which the liquid was replaced by the gases and accumulated in a graduated cylinder.

Apart from the thermal dechlorination pre-treatment, an additional experiment was employed to elucidate whether inorganic chlorine (e.g. salts) is present in the raw WEEE plastic. It was based on washing the raw plastic waste (WEEE) with MilliQ-H_2O at a H_2O/WEEE ratio of 20 ml/g of plastic. The mixture was stirred for 15 min plus 30 min in ultrasonic bath. After that, the washing water was analysed by Ion Chromatography (IC).

2.4. Plastic pyrolysis tests

Thermo-catalytic pyrolysis experiments were run in a downdraft fixed-bed stainless steel reactor with thermal and catalytic zones independently heated by two electrical furnaces. The schematic diagram of the experimental setup is reported elsewhere [32]. The internal temperatures were monitored by two K-type thermocouples placed in the char bed (thermal zone) and in the catalyst bed (catalytic zone). The two regions inside the reactor were physically separated by metallic tubes/plates and quartz wool.

All reactions were carried out at 600 ºC in the thermal zone, atmospheric pressure and, by using a 100 ml/min nitrogen flow as carrier and purging gas. In the catalytic pyrolysis assays, the catalyst-to-feedstock (C/F) ratio was equal to 0.2 and a temperature of 450 ºC was set on the catalytic zone.

Once the reactor reached the targeted temperatures, the sample was made to fall by opening the feeding valve. The reaction occurred through the formation of solid char, which was retained in the thermal zone, and primary pyrolysis vapours, that passed through the catalyst bed (if any) before exiting the reactor. At the end of the reaction, solid products (i.e., the char and the coke-containing catalyst) were independently collected for further characterisation. Oil, wax and gaseous fractions were collected by means of the condensation system and the water-containing column described in the previous section, respectively.

2.5. Analytical techniques

Inductively Coupled Plasma Optical Emission Spectrometry (ICP-OES) analysis was applied to measure the Al content in the prepared catalysts, as well as the chemical composition of the raw plastic ash. For the latter, the WEEE plastic was previously burned in a static oven up to 900 ºC in air flow, with a holding time of 30 min. For each ICP-OES analysis, a known amount of solid sample was first digested in an acidic solution of nitric and hydrofluoric acids (2:1 in volume), using an Anton Paar Multi-wave 3000 microwave. The obtained solution was then analysed employing a Perking Elmer Optima 7300AD instrument, feeding 1.5 ml/min of sample in 15 ml/min of argon as carrier gas.

The crystallinity of the zeolite catalysts, as well as of the polymers in the WEEE sample, was evaluated by powder X-Ray Diffraction analyses, employing a Philips X'Pert PRO diffractometer (Cu Kα radiation λ = 1.5406 Å, 40 kV, 30 mA). All the spectra were recorded in the 2θ range of 5 – 70°.

The morphology of the zeolite particles was investigated by means of a Field Emission Scanning Electron Microscopy (FE-SEM) model JEOL JSM-7900F (1.0-2.0Kv; detectors: Lower Electron Detector (LED) and Upper Electron Detector (UED)).

The textural properties of the investigated catalysts were determined by nitrogen physisorption at 77 K using an ASAP 2020 instrument from Micromeritics. Before the analysis, each sample was degassed at 350 ºC under vacuum for 6 h. The specific surface area was estimated by applying the Brunauer, Emmett and Teller (BET) equation [33]. Both the microporous volume and surface area were calculated by the t-plot method, using the Harkins and Jura equation [34]. The mesopore size distribution was determined by applying the Barrett–Joyner–Halenda (BJH) model to the adsorption branch of the isotherm.

Quantification of Brønsted and Lewis acid sites of the catalysts was carried out by adsorption of deuterated acetonitrile (CD_3CN) on their surface followed by FT-IR analysis in a Nicolet iS 10 – FTIR Spectrometer (Thermoscientific, USA), with 4 cm^{-1} optical resolution and a DTGS detector. For each measurement, about 25 mg of sample was pressed into a disk of 1.3 cm radius and then heated at 400 ºC (heating rate = 10 ºC/min, holding time = 2 h) and outgassed up to 10^{-5} torr. CD_3CN was subsequently adsorbed on the activated sample at 30 ºC for 30 min and the excess of basic probe was finally removed by vacuum evacuation at 10^{-5} torr for 10 h [35,36]. The FT-IR spectra were recorded in the range 4000 – 400 cm^{-1} and analysed by deconvolution through Peak Fit software, by using Gaussian curves and extinction factors of 2.05 and 3.60 cm/μmol to calculate the concentration of Brønsted and Lewis acid sites at 2325 and 2297 cm^{-1}, respectively [37].

Aluminium coordination in the zeolite samples was studied by ^{27}Al Magic Angle Spinning solid state Nuclear Magnetic Resonance (MAS NMR) on a Bruker Avance III spectrometer, supported with a 3.2 mm MAS probe, at 11.7 T. Spectra were recorded at room temperature at 15 kHz MAS. RF fields of 50 kHz and 40 kHz were used for the ^{27}Al $\pi/12$ pulse, followed by 26 ms acquisition. The number of scans accumulated was 10240, with a 1 s inter-scan delay. The ^{27}Al chemical shift was externally referred to an aqueous solution of aluminium nitrate. NMR spectra were analysed by deconvolution with Gaussian functions, and the curve areas were used to estimate the ratio between framework and extra-framework aluminium species.

The chlorine content in the raw and dechlorinated WEEE plastic, as well as in the pyrolysis products, was determined by oxidative combustion in a calorimetric bomb (AOD 1 Decomposition System by IKA), followed by Ion Chromatography (IC), according to DIN/EN 14582 and DIN 51527 standards. The IC chromatograph was a 30 Compact IC Flex from Metrohm having a Polyvinyl alcoholic with quaternary ammonium groups column (Metrosep A Supp 7 - 150/4.0) as stationary phase and using a sodium carbonate solution as eluent.

The ultimate analysis was performed on a Thermo Scientific FLASH 2000 CHNS/O micro-elemental analyser. The oxygen content was calculated by difference.

TG, DTG and DSC curves of the raw WEEE and the pre-treated samples were performed using a thermobalance (TA Instruments Q600 SDT) heating the sample up to 800 ºC at

10 ºC/min and maintaining this temperature for 10 min in nitrogen flow. Proximate analysis, as well as the coke determination in the spent catalysts, were performed by using the same thermobalance in air flow. Volatile matter was quantified from the weight loss of sample heated from room temperature to 900 ºC in Ar atmosphere (flow rate of 100 ml/min). The coke deposited on the spent catalysts was calculated from the weight change of the samples after combustion up to 850 ºC using an air flow of 100 ml/min and a heating rate of 10 ºC/min.

FT-IR analysis of raw and dechlorinated WEEE plastic was performed by using a Nicolett 6700 equipped with a diamond ATR crystal and a DTGS TEC detector. The spectra were collected in 550 – 4000 cm^{-1} range, with an optical resolution of 4 cm^{-1}, and by acquiring 64 scans.

The composition of the oil fraction was evaluated by PIONA analysis using a Gas Chromatograph Agilent 7890A, equipped with a CP-Sil PONA CB GC Column (100 m, 0.25 mm, 0.50 µm) and a Flame Ionisation Detector (FID). The samples were previously diluted in carbon disulfide (1 wt.%) and the equipment was calibrated with a multi-standard containing 360 different molecules in the range C_4 – C_{15}.

Pyrolysis gases were analysed in a dual channel Agilent CP-4900 Micro Gas Chromatograph, equipped with a Thermal Conductivity Detector (TCD) and using a He flow and two separation columns: molecular sieve (Molsieve 5 Å) and HayeSep A, respectively. Besides, it was calibrated for different concentrations of O_2, H_2, CO, CO_2, CH_4, C_2H_4, C_2H_6, C_3H_6, C_3H_8, C_4H_8, and C_4H_{10}.

From the experimental weight of each fraction (i), total mass balances were closed on the amount of plastic fed, according to the equation (2):

$$\text{Mass yield}_i\ (\%) = [\text{Mass}_i(g)/\ \text{Plastic Fed}\ (g)]\ *\ 100 \qquad (2)$$

For all the tests, the mass balances were closed over 95 %. High Heating Value (HHV) was calculated according to an empirical correlation valid for solid, liquid, and gaseous fuels, reported elsewhere [38].

3. Results and discussion

3.1. Catalyst characterisation

A total of three ZSM-5 zeolite samples were synthesised and thoroughly characterised, previous to their evaluation in the catalytic pyrolysis of the WEEE plastic waste. Two of such zeolites were prepared varying the Si/Al molar ratio (11 and 25), in order to evaluate the role of acidity in the overall catalytic pyrolysis process. The third sample was obtained from ZSM-5 (25) by means of a desilication treatment to introduce some mesoporosity in the intrinsically microporous zeolite.

Wide-angle XRD analyses (Figure 1A) revealed the characteristic pattern of MFI-type zeolites, denoting both good crystallinity and without detectable proportions of amorphous phase, even in the desilicated sample. ICP-OES analyses corroborated that their Si/Al ratios were very close to that of the starting synthesis gel (Table 1). Just in the case of ZSM-5 (25)_Des, a slightly lower value was reached compared to that of the parent zeolite due to the partial dissolution of the silica during the post-synthesis treatment.

^{27}Al MAS NMR analyses were carried out for the three zeolites to check whether all the aluminium was effectively incorporated in the zeolite framework. Figure 1B illustrates the resulting spectra, together with the calculated proportions of Al as framework (Al^{IV} at 54 ppm) and extra-framework (Al^{VI} at 0 ppm) species [39,40], as well as the Full Width at Half Maximum (FWHM) of Al^{IV}. As expected, most of the Al atoms are in the form of tetrahedral sites incorporated into the zeolite structure, although for the three samples the presence of a certain amount of extra-framework species is detected, which are probably extracted during the calcination process. The proportion of extra-framework aluminium (estimated as % relative area of the NMR peaks) increases with the Al content, following the trend: ZSM-5 (25) (8.0 %), ZSM-5 (25)_Des (11 %) and ZSM-5 (11) (17 %). The FWHM value of the framework Al peak is also higher for the sample with the lowest Si/Al ratio. This widening denotes changes in the T-O-T angles (T being Al or Si) and, therefore, a higher heterogeneity in the tetrahedral aluminium environment. It is remarkable that desilication induces structural changes in ZSM-5 (25), not only extracting more aluminium species, but also leading to the highest distortion of the framework Al environment, as denoted by the widest FWHM peak at 54 ppm.

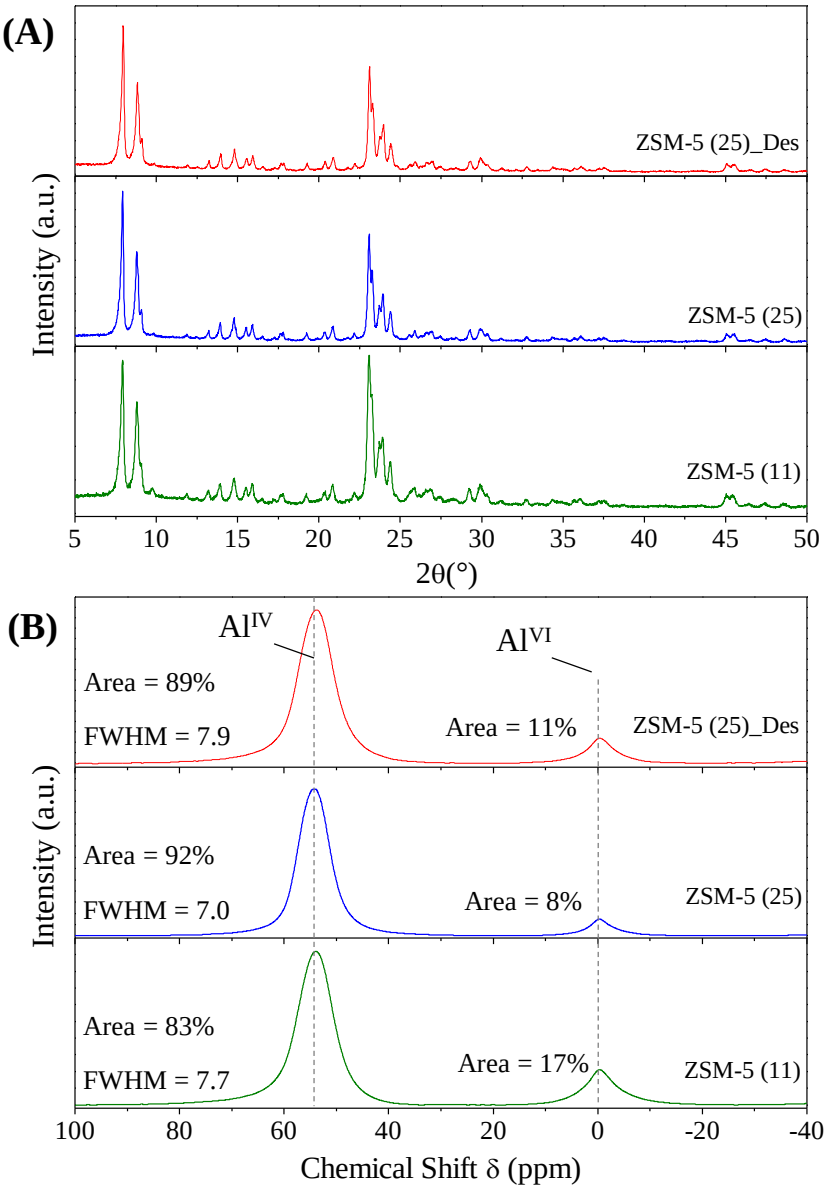

Figure 1. Wide-angle XRD patterns (A) and ^{27}Al MAS NMR spectra (B) of the ZSM-5 zeolites employed in the catalytic pyrolysis of WEEE. Within Fig. B the Full Width at Half Maximum (FWHM) of Al^{IV} and the relative area of the NMR peaks are given.

N_2 adsorption-desorption isotherms determined at 77 K, as well as BJH mesopore size distributions, are shown in Figure 2. In addition, Table 1 summarizes the main textural properties calculated from them, with values of S_{BET} typical of MFI zeolites (about 400 m^2/g). Desilication by alkaline treatment of ZSM-5 (25) zeolite induces a significant change in the shape of the isotherm, enhanced adsorption appearing at intermediate-high relative pressures. Moreover, a wide hysteresis loop, with almost parallel adsorption and desorption branches, can be observed for sample ZSM-5 (25)_Des, which is typically associated to open mesopores on the outer surface [41]. This fact is also reflected in the

BJH pore size distribution that evidences the presence of non-uniform mesopores with sizes in the range 50-200 Å and by the increase in the external/mesopore surface area.

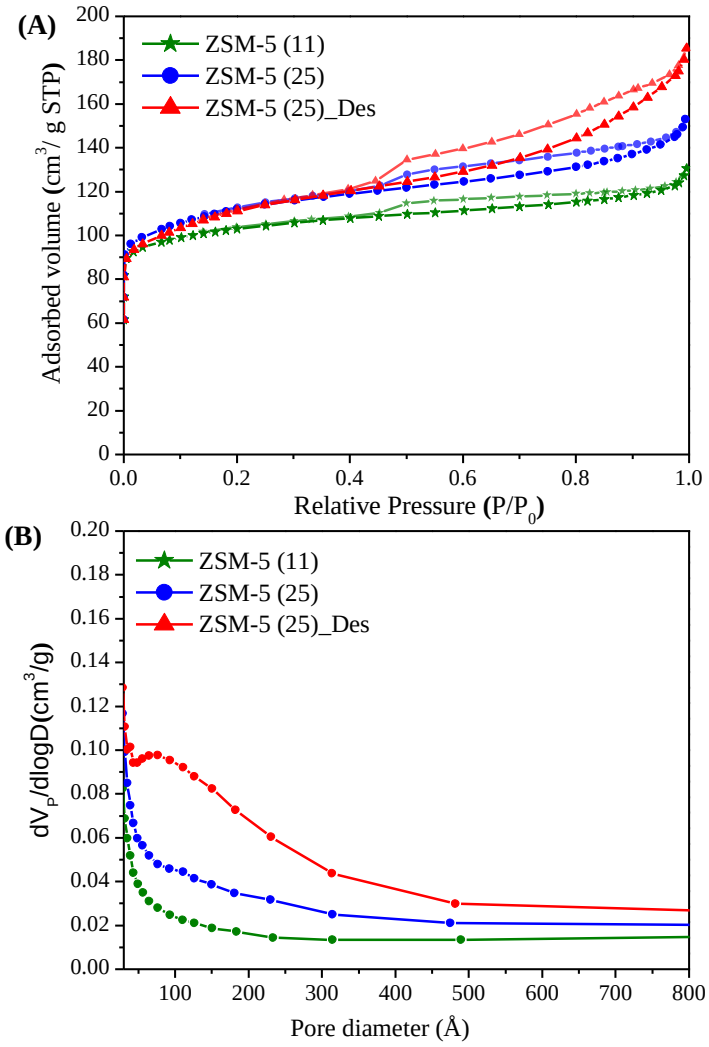

Figure 2. N_2 adsorption-desorption isotherms at 77 K (A) and BJH mesopore size distribution (B) of the ZSM-5 zeolites employed in the catalytic pyrolysis of WEEE.

Table 1. Textural properties and Si/Al ratios of the ZSM-5 samples.

Sample	**Si/Al[a] bulk (mol/mol)**	**S_{BET}[b] (m^2/g)**	**S_{mic}[c] (m^2/g)**	**$S_{ext-mes}$[c] (m^2/g)**	**V_{tot}[d] (cm^3/g)**	**V_{mic}[c] (cm^3/g)**	**$V_{ext-mes}$[e] (cm^3/g)**
ZSM-5 (11)	10.9	399	312	87	0.201	0.121	0.080
ZSM-5 (25)	23.6	418	283	135	0.233	0.114	0.119
ZSM-5 (25)_Des	21.7	407	241	166	0.281	0.099	0.182

[a] Determined by ICP-OES.
[b] BET specific surface area. [c] Calculated by t-plot method.
[d] Estimated at $p/p_0 = 0.98$. [e] Calculated by difference, $V_{tot} - V_{mic.}$

The effect of desilication applied to ZSM-5 (25) zeolite as generator of a secondary porosity was also corroborated by means of Scanning Electron Microscopy. As it can be seen in Figure 3, both the parent and desilicated zeolites are formed by spheroidal aggregates of interconnected crystals with the typical MFI coffin-shaped morphology. The voids existing within the aggregates of crystals may contribute with some mesoporosity in all samples, as observed in the textural properties of Table 1, this effect being more pronounced for the desilicated ZSM-5. At higher magnifications, some differences between both samples become evident in the SEM images. Thus, the crystals of the parent ZSM-5 (25) have a smooth external surface, while those of the desilicated zeolite show some roughness due to the partial dissolution of framework Si species.

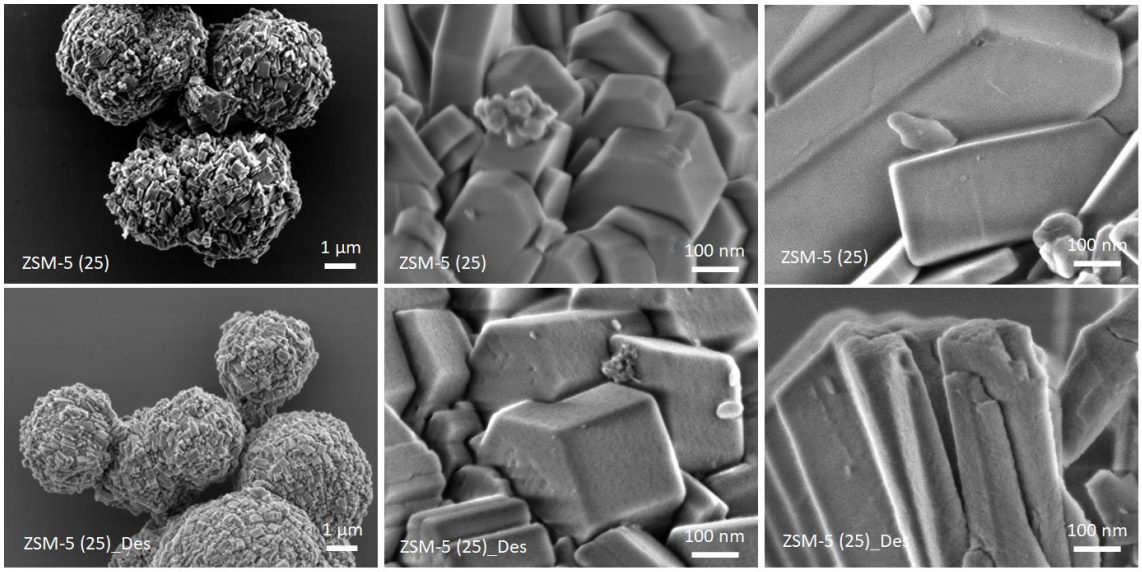

Figure 3. SEM images of ZSM-5 (25) and ZSM-5 (25)_Des zeolite samples at different magnifications.

In addition to textural properties, the acidity of the three zeolites was examined. In particular, the proportion of Lewis and Brønsted acid sites was determined by means of FT-IR analysis of the acetonitrile preadsorbed on the surface of the zeolites. The resultant values are presented in Table 2, while the FT-IR spectra and the deconvoluted curves are included in the Supporting Information (Figure S1). As expected, the highest total concentration of acid sites corresponds to ZSM-5 (11) and the lowest to ZSM-5 (25). However, both types of acidic sites do not keep proportionality between the samples, but Lewis ones increase to a greater extent at lower Si/Al ratios, which is consistent with the concentration of extra-framework Al species detected by ^{27}Al MAS NMR, in ZSM-5 (11)

higher than in ZSM-5 (25). It is remarkable that the desilicated zeolite exhibits the largest amount of Brønsted acidity. Despite there is an decrease in the Si/Al ratio and a higher percentage of extra-framework Al of this sample, they do not seem to fully justify the sharp increase in the Brønsted acidity. In this sense, an increase of Brønsted acidity has been reported previously and attributed to a partial reinsertion of previously extracted Al into zeolite framework positions close to the vacancies generated during desilication and, therefore, having a higher accessibility [41].

Table 2. Brønsted and Lewis acidity of the ZSM-5 zeolite samples.

Sample	ZSM-5 (11)	ZSM-5 (25)	ZSM-5 (25)_Des
Brønsted AS (μmol/g_{CAT})	488	378	523
Lewis AS (μmol/g_{CAT})	253	95	154
B/L ratio	1.93	3.98	3.4
Total AS (μmol/g_{CAT})	741	473	678

3.2. Properties of the raw and pre-treated WEEE waste

Firstly, in order to determine whether inorganic chlorine was present in the raw WEEE plastic, it was washed with H_2O-MilliQ. Ion Chromatography (IC) analysis of the washing-water showed an almost negligible Cl concentration (about 8 ppm of Cl referred to the weight of the plastic waste). This result reveals that the WEEE sample was not exposed to density separation methods using aqueous Cl salt solutions neither contaminated with any inorganic Cl source.

Once discarded the existence of inorganic chlorine in the WEEE sample, the effect of thermal dechlorination pre-treatment on the composition, structure and thermal properties of WEEE was assessed.

Figure S2 illustrates the XRD analyses of the WEEE plastic and that corresponding to the pre-treated feedstock. The peaks centred at 2θ of 22º, 24° and 36º correspond to the PE inter planner spacings of 4.132, 3.707 and 2.481 Å, respectively, which fit to the (110), (200) and (020) lattice planes. These data indicate that the WEEE waste contains crystalline PE with orthorhombic structure [42]. In addition, a broad band centred at 2θ = 20.4° denotes also the occurrence of amorphous PE phases [43]. According to literature, PVC shows XRD peaks at 2θ = 17º and 24.5°, but they are hardly distinguished in Figure S2 as they overlap with signals of the PE polymer, which is predominant in the WEEE

waste. Moreover, no significant differences can be appreciated between the XRD patterns of the WEEE feedstock before and after the thermal pre-treatment at 350 ºC, indicating that the latter does not affect to the ratio of crystalline/amorphous phases in the PE polymer.

Proximate and elemental analysis of both raw WEEE and pre-treated samples were performed to determine their chemical composition, which are summarised in Table 3. Proximate analyses of the samples were pretty similar, as both materials lose about 97 – 98 wt.% of volatiles with a remaining ash content below 3 wt.%, which corresponds probably with inorganic additives incorporated to the polymers.

Table 3. Proximate and ultimate analyses of raw and thermally dechlorinated WEEE.

Proximate Analysis (wt.%)				**Elemental Analysis (wt.%)**						
Sample	Volatiles[a]	Fixed C[b]	Ash[c]	C	H	N	Cl[d]	Trace metals[e]	O[b]	HHV (MJ/kg)
Raw WEEE	97.2	0	2.8	78.0	13.3	0.0	1.95 ±0.48	0.9	4.0	42.4
Pre-treated WEEE	97.6	0	2.4	82.0	14.1	0.0	0.26 ±0.04	0.9	1.2	45.1

[a] Quantified by TGA at 900ºC in Ar; [b] Calculated by difference; [c] Measured by combustion in a muffle furnace at 900ºC; [d] Analysed by AOD/IC; [e] Measured by ICP-OES of ashes.

Regarding the ash composition of WEEE sample, Table 4 summarizes the main elements that were detected, showing that the feedstock contains significant amounts of Ti, Si and Ca, followed by Cu, Al, Na, Mg and Zn. These inorganic components can be related mainly to the incorporation of fillers and additives (such as TiO_2, SiO_2 and CaO) to the polymers for improving their properties. Nevertheless, contamination of the plastics during their use can also contribute to some of these inorganic species.

Table 4. ICP-OES analysis of ash from WEEE plastic sample.

Trace Metal	**Concentration (ppm)**	**Trace Metal**	**Concentration (ppm)**
Ti	3,360.1	Zn	117.9
Si	2,041.0	Sn	82.7
Ca	2,020.5	K	58.6
Cu	571.5	Fe	49.9
Al	372.8	B	48.3
Na	263.5	P	46.6
Mg	168.3	Pb	34.5

The Cl content of the WEEE sample, measured by AOD-IC (Table 3), was 1.95±0.48 wt.%, which is assumed to arise mainly from the presence of PVC in the WEEE plastic (with a proportion at about 3.44±0.85 wt.%), the remaining polymer corresponding to PE. The relatively large standard deviation in the determination of the Cl content can be assigned to the high heterogeneity of the raw plastic waste even after milling. Regarding the pre-treated sample, its Cl content was reduced significantly reaching a value of 0.26±0.04 wt.% of Cl. This result would correspond with about 87 % efficiency in the removal of Cl during the thermal pre-treatment. However, this number should be assessed carefully, as it implies that the pre-treated WEEE feedstock still contains a relatively high concentration of Cl (0.26 wt.%, i.e. 2,600 ppm), hindering its further processing. This finding agrees well with previous literature works that also identified the Cl presence after mild thermal treatment of PVC-containing materials [28,44–46]. Thus, McNeill et al. suggested that a small amount of hydrogen chloride could be retained by the polymer once polyenes are present giving rise to chlorinated hydrocarbons [47]. On the other hand, different authors have suggested that PVC can suffer photo-oxidation during its lifetime [48,49], leading to the formation of oxygenated Cl-containing groups (photoproducts), such as acyl chloride, β-chlorocarboxylic acid, α,ά-dichloro ketone and β-chloro anhydride [49]. These species could be responsible for the remaining Cl in the pre-treated material. In this way, the presence of oxygen (4.0 and 1.2 wt.%) in both raw and pre-treated samples could be considered an indication of the photo-oxidation suffered by the polymers (PE and PVC) contained in this real WEEE plastic waste during their lifetime (as cables).

Figure 4(A) displays the TG/DTG analyses of both the raw WEEE plastic and the pre-treated sample under inert atmosphere. The occurrence of a peak at about 284.4 ºC in the DTG curve of the raw plastic waste is a clear indication of the PVC presence, being originated by the release of HCl. From several repetitions of the TG measurements, an average weight loss between 200 and 350 ºC of 3.36±0.9 wt.% has been obtained, which would correspond to a PVC content in the raw WEEE of 5.8±1.5 wt.%. Although this value is somewhat higher than that obtained from the AOD-IC measurements (3.44±0.85 wt.%), it can be considered a reasonable result taking into account the great heterogeneity of the raw plastic waste and the small amount of sample (10-20 mg) employed in the TG tests. Moreover, elimination of additives and oxygenated compounds generated by photo-oxidation processes can be interfering during this weight loss stage at temperature

below 300°C. Pan et al.[50] detected also other compounds (e.g. 1,3-butadiene or benzene) released at this temperature range from PVC, leading to an overestimation of the PVC content. Accordingly, for the rest of the work, the Cl (and PVC) contents estimated from the AOD-IC analyses have been considered as more accurate.

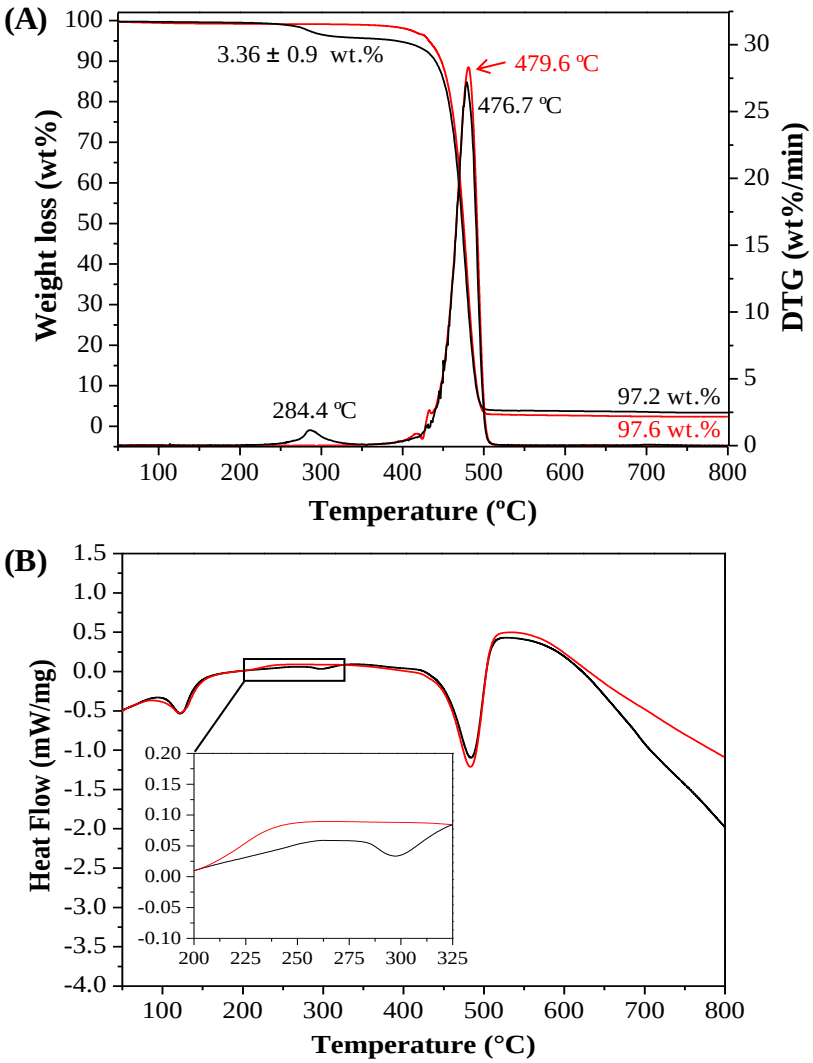

Figure 4. Thermal characterization of raw WEEE (black solid) and pre-treated (red dash) feedstocks under inter atmosphere: TG and DTG curves from thermogravimetric analysis (A) and Heat Flow from differential scanning calorimetry (B).

According to the literature, the second step of PVC thermal decomposition occurs between 400 and 520 ºC trough the cracking of C–C bonds in the remaining polymeric solid. However, this transformation cannot be distinguished in the TG curve of Figure 5 as it overlaps with the PE decomposition [44,51,52]. Thus, the peak maximum of this step for both samples is placed at around 477–480 ºC, which matches well with the PE thermal

cracking [53]. On the other hand, the pre-treated feedstock does not show any relevant weight loss below 400 ºC, which, a priori, would suggest that a high dechlorination degree has been achieved during the pre-treatment. These differences between raw and pre-treated plastic sample are also appreciated in Figure 4(B). In this sense, the endothermal degradation of the PVC and the release of HCl can be clearly observed in the raw sample spanning a range of temperatures between 275-375 ºC. This signal is practically absent in the pre-treated plastic waste, denoting again that no PVC fragments remains in this material.

Figure 5(A) displays the FT-IR analyses of both raw WEEE and thermally pre-treated samples. Both spectra are almost a copy of the fingerprint of PE (as it represents > 95 wt.% of the raw sample), showing the absorption bands corresponding to C-H stretching at 2849 and 2916 cm^{-1}, CH_2 bending at 1472-1462 cm^{-1}, CH_2 rocking at 730-717 cm^{-1}, and a small band at 1379 cm^{-1} related to CH_3 bending. Most of the bands associated to the C-Cl stretching (840-637 cm^{-1}) in pure PVC [54] are not obvious in the raw WEEE sample due to the small share of PVC. The absorbance band at 1726 cm^{-1} detected in the inset of FT-IR spectra of the raw WEEE residue is observable in the spectra of commercial PVC resins [55,56]. It is usually attributed to hydrogen bonded C=O groups of different acrylic processing aids used as promoters to modify PVC properties (plasticisation, fusion temperature, melt rheology modification or lubrication, among others). However, such band fully disappears after thermal pre-treatment of the sample, in agreement with the reduction observed in the oxygen concentration of the pre-treated sample. On the other hand, the inset in FT-IR spectra of the pre-treated sample shows that a small signal at 1625-1650 cm^{-1} emerges, which could be ascribed to the C=C bonds formed as a consequence of dechlorination of PVC [56].

In order to discern with more clarity the changes in PVC composition induced by the pre-treatment, particles identified in the raw WEEE waste as being mainly composed by this polymer were manually separated and analysed by FT-IR before and after the thermal pre-treatment (Figure 5(B)). The main absorption bands in the raw sample agree rather well with those of pure PVC [46,56,57], demonstrating that the isolated particles mainly consists of this polymer. After the thermal pre-treatment most of the bands associated to the presence of chlorine disappear, including those at 2970 cm^{-1} (C-H stretching of CHCl) and 1255 cm^{-1} (C-H deformation of CHCl). In addition, other typical bands of PVC, not directly related with chlorine, such as 1100-1070 cm^{-1} (C-C stretching) and 966 cm^{-1} (CH_2

rocking), disappear, whereas a new band at 1625 cm^{-1} (C=C bond stretching) arises due to the formation of vinyl groups during the PVC dechlorination [46]. On the other hand, the band attributed to hydrogen bonded C=O groups (1726 cm^{-1}), arising mostly from PVC plasticisers, is more noticeable than in the raw WEEE, being also fully disappeared after the thermal pre-treatment [56,57]. Furthermore, the PVC-containing sample before and, especially after the thermal treatment, shows also a broad band at ≈ 3500 cm^{-1} due to the ambient hydration of the sample [57].

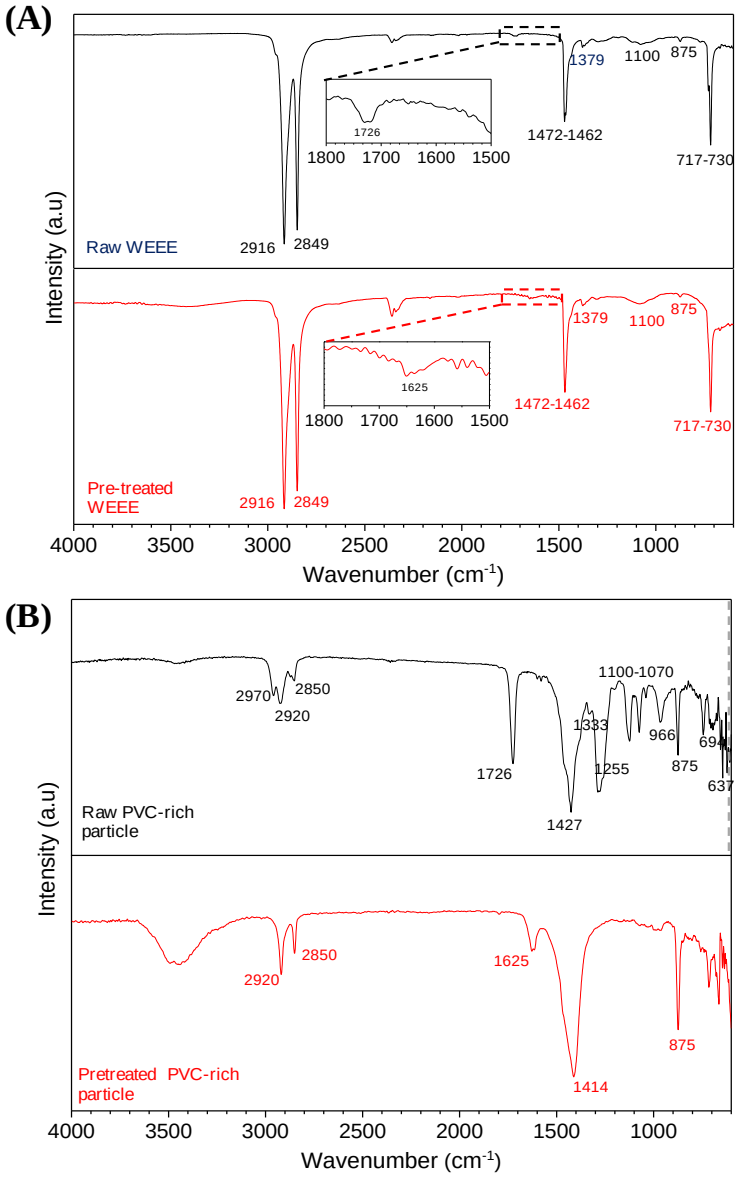

Figure 5. FT-IR spectra of raw WEEE and pre-treated feedstocks (A), and of particles intentionally isolated from raw and pre-treated mainly composed of PVC (B).

3.3. WEEE catalytic pyrolysis tests

The three ZSM-5 samples were tested as catalysts for the conversion of the WEEE plastic using an ex-situ configuration, in which the plastic is first thermally decomposed in the upper part of the reaction system and the so generated vapours are then passed through the zeolite bed, being catalytically upgraded. The temperatures selected for the thermal/catalytic zones were 600 and 450 ºC, respectively. In addition, a pure thermal test, with no catalyst, was performed as reference. The following product fractions were collected: char (solid product remaining in upper part of the reactor), coke (carbonaceous residue deposited on the catalyst), wax (solid fraction recovered at the exit of the reactor), oil (liquid phase recovered by condensation) and gases.

The product distribution per fraction obtained in these tests is represented in Figure 6. In all cases, the char yield was very similar (about 8 – 9 wt.%), which is an expected result as this fraction is accumulated in the thermal zone of the reactor, i.e., before entering into contact with the catalyst. In the thermal test, the largest product corresponded with the wax fraction, whereas just minor amount of oil and gases were generated. Wax is assumed to be formed by a random cracking mechanism occurring at any point in the polymeric chains [5]. This product distribution sharply changed in the presence of the ZSM-5 catalysts that led to a strong enhancement in the yield of oil and gases. Moreover, for two of the samples (ZSM-5 (25) and ZSM-5 (25)_Des), the wax fraction completely disappeared, denoting the high activity of these materials for further cracking long-chain hydrocarbons into lighter components. Nevertheless, a significant proportion of wax (about 30 wt.% yield) was still present among the catalytic pyrolysis products when using the ZSM-5 (11) sample. This result indicates the lower activity of this sample, which can be assigned to a combination of factors, such as its higher content of extra-framework Al species and its higher share of Lewis acid sites, which are expected to exhibit lower intrinsic cracking activity in comparison with the Brønsted acidity. Moreover, this sample is more prone to coke formation and, therefore, to suffer catalyst deactivation. On the other hand, a remarkable result is that the oil becomes the predominant phase for the other two zeolite samples, reaching yields over 60 wt.%.

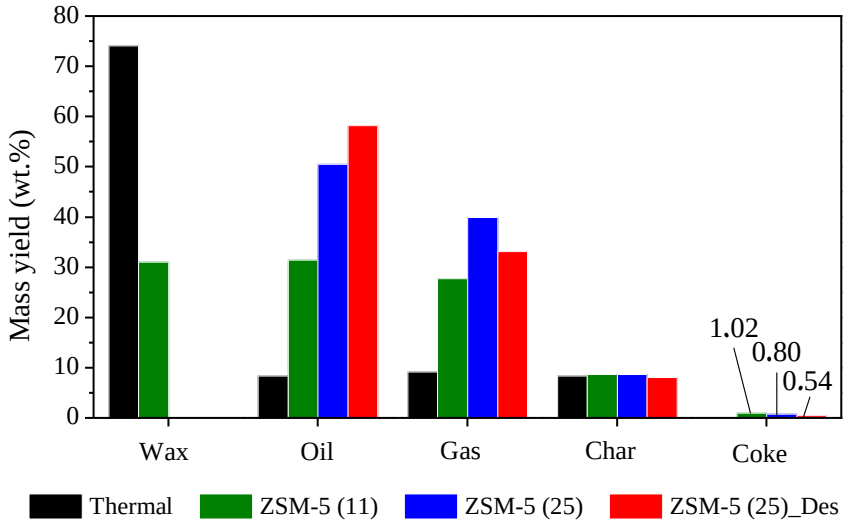

Figure 6. Thermal and catalytic pyrolysis of pre-treated WEEE: product distribution per fractions. Reaction conditions: 600/450 ºC (thermal/catalytic zone); C/F ratio = 0.2.

Figure 7 provides the yield of the different components, mainly hydrocarbons, detected in the gaseous stream. Minor amounts of CO_2 and CO are present in the gases, which is consistent some oxygen still remaining in the pre-treated plastic waste, whereas hydrogen is produced in very low amounts, and mainly in the catalytic tests as the ZSM-5 zeolite promotes dehydrogenation reactions. Nevertheless, the highest impact derived from the presence of the catalysts is noticed in the formation of light hydrocarbons, inducing a sharp increase in the yield of both gaseous olefins and paraffin yields, due to the extension of end-chain cracking reactions [5,58]. In contrast, the production of methane is little affected, showing that the latter is formed mainly by thermal processes. ZSM-5 (11) leads to lower yields of both light olefins and paraffins compared to the other two zeolite samples, confirming the lower cracking activity of the former.

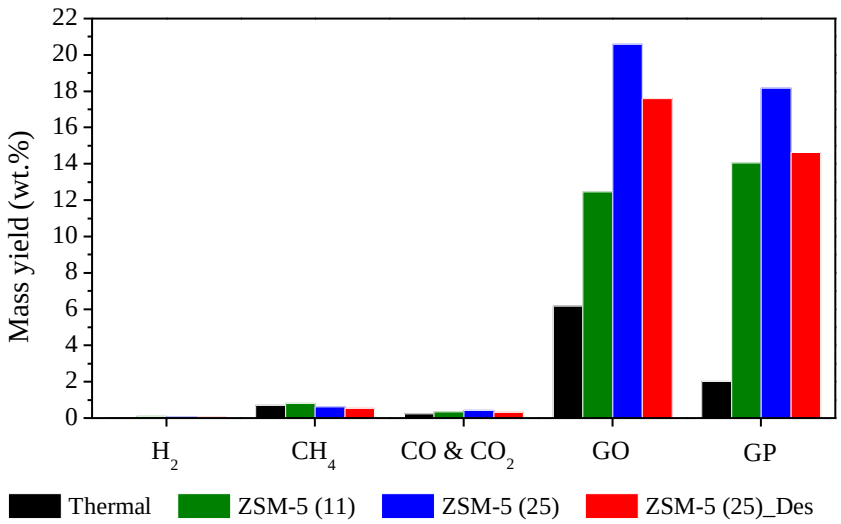

Figure 7. Thermal and catalytic pyrolysis of pre-treated WEEE: mass yield of the gaseous products. Reaction conditions: 600/450 ºC (thermal/catalytic zone); C/F ratio = 0.2

Figure 8(A) illustrates the whole product distribution of hydrocarbons, in terms of selectivity, for the two zeolite catalysts showing the highest activity. Very similar profiles are obtained in both cases, consisting of a bimodal distribution with two peaks. The first one is placed at C_3 – C_4, being related to end-chain cracking reactions catalysed mainly by the strong Brønsted acid sites of the ZSM-5 zeolites. The second peak is observed at C_8, with a significant share also of C_6 and C_7 hydrocarbons. Based on previous works of polyolefin catalytic cracking [5,58,59], C_6 – C_8 components can be related with the occurrence of secondary transformations of the light olefins produced in the primary cracking reactions that, subsequently, undergo the oligomerisation/cyclisation/aromatisation pathway. This is confirmed by the PIONA analyses of the oil fraction (Figure 8B), which denote that aromatic hydrocarbons are by large the major components of the liquids obtained by catalytic pyrolysis of the WEEE plastic waste. Thus, the content of mono-aromatic hydrocarbons (mainly BTX) in the oil fraction is over 50 wt.% for both zeolites. This is a remarkable result as these compounds can be used for the formulation of gasoline-range fuels due to their high RON number, as well as raw chemicals. This last option would be of high interest as it would imply the chemical recycling of the plastic waste instead of just energy recovery.

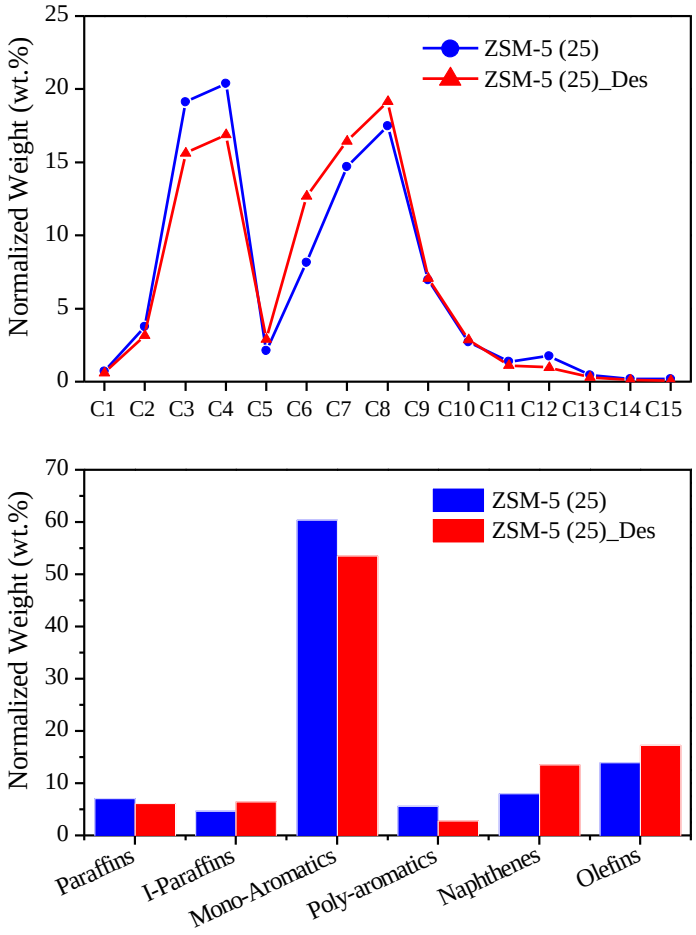

Figure 8. Catalytic pyrolysis of pre-treated WEEE: distribution of hydrocarbons per atom carbon number (A) and PIONA analyses (B) of the oils obtained with ZSM-5 (25) and ZSM-5 (25)_Des. Reaction conditions: 600/450 ºC (thermal/catalytic zone); C/F ratio = 0.2

Since the plastic feedstock still contains a significant amount of Cl (about 0.26 wt.%) even after the pre-treatment at 350 ºC, an important fact is how this halogen is distributed among the different fractions of the pyrolysis process. In this way, it must be noted that the presence of Cl concentrations in the oil over 100 ppm may preclude the further feeding and processing of this fraction in refinery facilities. Accordingly, the halogen content of all the pyrolysis fractions has been quantified by AOD-IC technique, the results so obtained being summarised in Table 5. The overall Cl mass balance is closed in the range 91.4 – 117.7 %, which can be considered a relatively accurate result taking into account the heterogeneity of the raw plastic waste, formed by a mixture of PE and PVC, which leads to a significant dispersion in the determination of its Cl content. In all tests, the char fraction accumulates most of the chlorine, which may be related to the presence of some

inorganic components, like Ca-containing compounds, that are known to be able of forming the corresponding chlorides. The next fraction in terms of Cl content is the wax, followed by the oil and, finally, the gases. In fact, the Cl detected in the gases as HCl is practically negligible. In this way, it must be taken into account that, during the thermal pre-treatment applied to the feedstock, a large part of the Cl originally contained in the raw plastic waste has been already removed as HCl.

Table 5. Cl distribution in the pyrolysis fractions determined by AOD-IC (referred to the average Cl content of the pre-treated WEEE plastic waste).

Sample	**Cl Balance (wt.%)**					
	Wax	**Oil**	**Gas[b]**	**Char**	**Coke**	**Total**
Thermal	5.2	0.0[a]	0.2	93.9	0.0	99.3
ZSM-5 (11)	14.4	8.7	0.1	91.6	2.8	117.7
ZSM-5 (25)	-	4.5	0.1	91.3	2.9	98.8
ZSM-5 (25)_Des	-	1.7	0.2	85.2	4.3	91.4

[a] No oil was recovered.

[b] Chlorine in the gases, collected in water traps.

The relative concentration of Cl in the different fractions is represented in Figure 9. Char presents Cl concentrations above 20,000 ppm, showing a significant variation among the experiments, which can be again assigned to the great heterogeneity of the raw plastic waste. The following fraction in terms of Cl concentration is the coke deposited on the catalyst, the highest value being observed for the desilicated zeolite. This finding suggests that the presence of mesoporosity in this material favours the trapping of bulky Cl-containing species, which in contrast is more difficult to take place on the other two zeolites. The rest of the Cl is distributed between the wax and the oil fractions. In the last case, remarkable differences are observed between the three zeolite samples, the lowest value being obtained over ZSM-5 (25)_Des, which can be related to the good performance of this material for trapping Cl-containing species within the carbonaceous matter deposited on the catalyst. As a consequence, the oil produced with this sample shows a Cl content below 100 ppm, which is the limit usually imposed by refineries to process this type of streams.

The picture coming from these results is that the Cl remaining in the WEEE plastic waste after the thermal pre-treatment is released during the pyrolysis process mainly in the form of bulky Cl-containing species that, therefore, tend to be accumulated in the heavier fractions, such as char and coke. Moreover, if any HCl is formed during the pyrolysis process, it should be fast captured by the mineral matter contained in the char, hence almost no HCl is detected in the produced gases. Finally, the oil dechlorination degree of the ZSM-5 zeolites seems to be directly related with their external/mesopore surface area since it may favour the trapping of the bulky Cl-containing compounds.

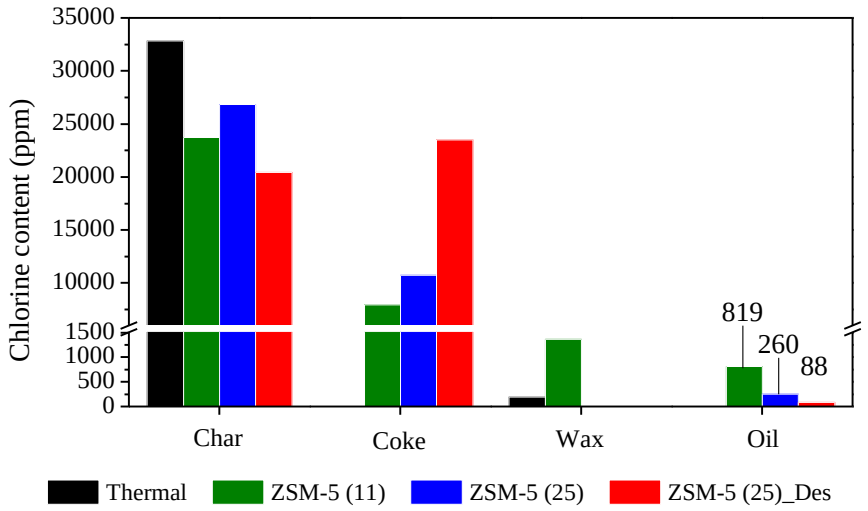

Figure 9. Thermal and catalytic pyrolysis of pre-treated WEEE: Cl concentration in the different fractions. Reaction conditions: 600/450 ºC (thermal/catalytic zone); C/F ratio = 0.2

4. Conclusions

The thermochemical processing of a real chlorinated plastic waste from the electric and electronic equipment sector (WEEE) into valuable products has been evaluated by catalytic pyrolysis over ZSM-5 zeolites. This waste comes from the recovery of electric cables and consists of a PE/PVC mixture (about 3.4 wt.% PVC) in addition to both organic and inorganic additives.

The effectiveness of the WEEE feedstock thermal pre-treatment herein employed (350 ºC for 30 minutes) was evaluated, resulting in a chlorine removal of 87% in the form of HCl, which also caused a significant reduction in its oxygen content. It is envisaged that the possible photo-oxidation suffered by the WEEE plastic wastes during their lifetime

could hinder to reach a total dehydrochlorination of the feedstock during this mild thermal pre-treatment.

The pre-treated sample was pyrolysed in a downdraft fixed-bed reactor to evaluate the catalytic performance of three ZSM-5 zeolite samples showing different properties in terms of acidity and accessibility. Thermal pyrolysis produces mainly waxes, while the catalytic tests using the ZSM-5 samples significantly altered the products distribution, allowing the conversion of the wax fraction into oil and gases. The desilicated ZSM-5 sample exhibited a convenient combination of acidity and accessibility, thanks to the additional mesoporosity created by the desilication post-treatment, being the material producing the largest oil yield (about 60 wt.%). Interestingly, the concentration of monoaromatics (mainly BTX) in this oil was over 50 wt.%, opening the way for its use in the formulation of raw chemicals in addition to fuels.

The chlorine distribution in the pyrolysis products was assessed in detail as the pre-treated WEEE feedstock still contains a significant amount of Cl (about 2,600 ppm). About 90% of the Cl is retained in the char fraction probably due to the presence in the ash of inorganic components that may act as halogen traps. Moreover, a relatively high concentration of Cl is also detected in the coke deposited on the catalyst, followed by the wax and oil fractions, whereas almost no chlorine is detected in the gaseous fractions. These results suggest the presence of heavy Cl-containing compounds. The lowest concentration of Cl in the oil was attained with the desilicated zeolite, with a value of 88 ppm, affording its further upgrading and processing in refinery units.

Acknowledgements

A.M. is grateful to the financial support by the Italian Ministry of University and Research (MUR), grant by PON-RI 2014-2020 (CCI 2014IT16M2OP005).

References

[1] L. Esposito, L. Cafiero, D. De Angelis, R. Tuffi, S. Vecchio Ciprioti, Valorization of the plastic residue from a WEEE treatment plant by pyrolysis, Waste Manag. 112 (2020) 1–10. doi:10.1016/j.wasman.2020.05.022.

[2] G.F. Cardamone, F. Ardolino, U. Arena, About the environmental sustainability of the European management of WEEE plastics, Waste Manag. 126 (2021) 119–132. doi:10.1016/j.wasman.2021.02.040.

[3] Y. Shen, R. Zhao, J. Wang, X. Chen, X. Ge, M. Chen, Waste-to-energy: Dehalogenation of plastic-containing wastes, Waste Manag. 49 (2016) 287–303. doi:10.1016/j.wasman.2015.12.024.

[4] K. Ragaert, L. Delva, K. Van Geem, Mechanical and chemical recycling of solid plastic waste, Waste Manag. 69 (2017) 24–58. doi:10.1016/j.wasman.2017.07.044.

[5] D.P. Serrano, J. Aguado, J.M. Escola, Developing advanced catalysts for the conversion of polyolefinic waste plastics into fuels and chemicals, ACS Catal. 2 (2012) 1924–1941. doi:10.1021/cs3003403.

[6] C. Santella, L. Cafiero, D. De Angelis, F. La Marca, R. Tuffi, S. Vecchio Ciprioti, Thermal and catalytic pyrolysis of a mixture of plastics from small waste electrical and electronic equipment (WEEE), Waste Manag. 54 (2016) 143–152. doi:10.1016/j.wasman.2016.05.005.

[7] A. López, I. de Marco, B.M. Caballero, M.F. Laresgoiti, A. Adrados, A. Aranzabal, Catalytic pyrolysis of plastic wastes with two different types of catalysts: ZSM-5 zeolite and Red Mud, Appl. Catal. B Environ. 104 (2011) 211–219. doi:10.1016/j.apcatb.2011.03.030.

[8] D.P. Serrano, J. Aguado, J.M. Escola, J.M. Rodriguez, A. Peral, Hierarchical zeolites with enhanced textural and catalytic properties synthesized from organofunctionalized seeds, Chem. Mater. 18 (2006) 2462–2464. http://dx.doi.org/10.1021/cm060080r.

[9] M.S. Holm, E. Taarning, K. Egeblad, C.H. Christensen, Catalysis with hierarchical zeolites, Catal. Today. 168 (2011) 3–16. doi:10.1016/j.cattod.2011.01.007.

[10] M. Alonso-Doncel, A. Peral, C. Ochoa-Hernández, R. Sanz, D.P. Serrano, Tracking the evolution of embryonic zeolites into hierarchical ZSM-5, J. Mater. Chem. A. 9 (2021) 13570–13587.

[11] Y. Zang, J. Wang, J. Gu, J. Qu, F. Gao, M. Li, Cost-effective synthesis of hierarchical HZSM-5 with a high Si/TPA+ ratio for enhanced catalytic cracking of polyethylene, J. Solid State Chem. 291 (2020) 121643. doi:10.1016/j.jssc.2020.121643.

[12] K.A. Tarach, K. Góra-Marek, J. Martinez-Triguero, I. Melián-Cabrera, Acidity and accessibility studies of desilicated ZSM-5 zeolites in terms of their effectiveness as catalysts in acid-catalyzed cracking processes, Catal. Sci. Technol. 7 (2017) 858–873. doi:10.1039/c6cy02609e.

[13] A. Coelho, L. Costa, M.M. Marques, I.M. Fonseca, M.A.N.D.A. Lemos, F. Lemos, The effect of ZSM-5 zeolite acidity on the catalytic degradation of high-density polyethylene using simultaneous DSC/TG analysis, Appl. Catal. A Gen. 413–414 (2012) 183–191. doi:10.1016/j.apcata.2011.11.010.

[14] J. Yu, L. Sun, C. Ma, Y. Qiao, H. Yao, Thermal degradation of PVC: A review, Waste Manag. 48 (2016) 300–314. doi:10.1016/j.wasman.2015.11.041.

[15] R. Miranda, J. Yang, C. Roy, C. Vasile, Vacuum pyrolysis of PVC I. Kinetic study, Polym. Degrad. Stab. 64 (1999) 127–144. doi:10.1016/S0141-3910(98)00186-4.

[16] D. Li, S. Lei, P. Wang, L. Zhong, W. Ma, G. Chen, Study on the pyrolysis behaviors of mixed waste plastics, Renew. Energy. 173 (2021) 662–674. doi:10.1016/j.renene.2021.04.035.

[17] Y. Wang, K. Wu, Q. Liu, H. Zhang, Low chlorine oil production through fast pyrolysis of mixed plastics combined with hydrothermal dechlorination pretreatment, Process Saf. Environ. Prot. 149 (2021) 105–114. doi:10.1016/j.psep.2020.10.023.

[18] L. Ye, T. Li, L. Hong, Understanding enhanced char formation in the thermal decomposition of PVC resin: Role of intermolecular chlorine loss, Mater. Today Commun. 26 (2021) 102186. doi:10.1016/j.mtcomm.2021.102186.

[19] T. Bhaskar, M. Tanabe, A. Muto, Y. Sakata, C.F. Liu, M. Der Chen, C.C. Chao,

Analysis of chlorine distribution in the pyrolysis products of poly(vinylidene chloride) mixed with polyethylene, polypropylene or polystyrene, Polym. Degrad. Stab. 89 (2005) 38–42. doi:10.1016/j.polymdegradstab.2004.12.022.

[20] T. Bhaskar, R. Negoro, A. Muto, Y. Sakata, Prevention of chlorinated hydrocarbons formation during pyrolysis of PVC or PVDC mixed plastics, Green Chem. 8 (2006) 697–700. doi:10.1039/b603037h.

[21] N. Miskolczi, L. Bartha, A. Angyal, Pyrolysis of polyvinyl chloride (pvc)-containing mixed plastic wastes for recovery of hydrocarbons, Energy and Fuels. 23 (2009) 2743–2749. doi:10.1021/ef8011245.

[22] P.T. Williams, E.A. Williams, Interaction of plastics in mixed-plastics pyrolysis, Energy and Fuels. 13 (1999) 188–196. doi:10.1021/ef980163x.

[23] S. Uçar, S. Karagöz, T. Karayildirim, J. Yanik, Conversion of polymers to fuels in a refinery stream, Polym. Degrad. Stab. 75 (2002) 161–171. doi:10.1016/S0141-3910(01)00215-4.

[24] B. Fekhar, N. Miskolczi, Stability and storage properties of hydrocarbons obtained by pilot scale pyrolysis of real waste HDPE-PVC in tubular reactor, Chem. Eng. Trans. 70 (2018) 1141–1146. doi:10.3303/CET1870191.

[25] A. Lopez-Urionabarrenechea, I. De Marco, B.M. Caballero, M.F. Laresgoiti, A. Adrados, Catalytic stepwise pyrolysis of packaging plastic waste, J. Anal. Appl. Pyrolysis. 96 (2012) 54–62. doi:10.1016/j.jaap.2012.03.004.

[26] Y.H. Lin, M.H. Yang, Catalytic reactions of post-consumer polymer waste over fluidised cracking catalysts for producing hydrocarbons, J. Mol. Catal. A Chem. 231 (2005) 113–122. doi:10.1016/j.molcata.2005.01.003.

[27] J. Lei, G. Yuan, P. Weerachanchai, S.W. Lee, K. Li, J.Y. Wang, Y. Yang, Investigation on thermal dechlorination and catalytic pyrolysis in a continuous process for liquid fuel recovery from mixed plastic wastes, J. Mater. Cycles Waste Manag. 20 (2018) 137–146. doi:10.1007/s10163-016-0555-3.

[28] A. López, I. De Marco, B.M. Caballero, M.F. Laresgoiti, A. Adrados, Dechlorination of fuels in pyrolysis of PVC containing plastic wastes, Fuel Process. Technol. 92 (2011) 253–260. doi:10.1016/j.fuproc.2010.05.008.

[29] M. Migliori, A. Aloise, G. Giordano, Methanol to dimethylether on H-MFI

catalyst: The influence of the Si/Al ratio on kinetic parameters, Catal. Today. 227 (2014) 138–143. doi:10.1016/j.cattod.2013.09.033.

[30] M. Migliori, A. Aloise, E. Catizzone, G. Giordano, Kinetic analysis of methanol to dimethyl ether reaction over H-MFI catalyst, Ind. Eng. Chem. Res. 53 (2014) 14885–14891. doi:10.1021/ie502775u.

[31] A. Aloise, A. Marino, F. Dalena, G. Giorgianni, M. Migliori, L. Frusteri, C. Cannilla, G. Bonura, F. Frusteri, G. Giordano, Desilicated ZSM-5 zeolite: Catalytic performances assessment in methanol to DME dehydration, Microporous Mesoporous Mater. 302 (2020) 110198. doi:10.1016/j.micromeso.2020.110198.

[32] J. Fermoso, H. Hernando, S. Jiménez-Sánchez, A.A. Lappas, E. Heracleous, P. Pizarro, J.M. Coronado, D.P. Serrano, Bio-oil production by lignocellulose fast-pyrolysis: Isolating and comparing the effects of indigenous versus external catalysts, Fuel Process. Technol. 167 (2017) 563–574. doi:10.1016/j.fuproc.2017.08.009.

[33] J. Rouquerol, P. Llewellyn, F. Rouquerol, Is the BET equation applicable to microporous adsorbents?, Elsevier B.V., 2007. doi:10.1016/s0167-2991(07)80008-5.

[34] M. Thommes, K. Kaneko, A. V. Neimark, J.P. Olivier, F. Rodriguez-Reinoso, J. Rouquerol, K.S.W. Sing, Physisorption of gases, with special reference to the evaluation of surface area and pore size distribution (IUPAC Technical Report), Pure Appl. Chem. 87 (2015) 1051–1069. doi:10.1515/pac-2014-1117.

[35] M. Trombetta, A. Gutièrrez Alejandre, J. Ramirez Solis, G. Busca, An FT-IR study of the reactivity of hydrocarbons on the acid sites of HZSM5 zeolite, Appl. Catal. A Gen. 198 (2000) 81–93. doi:10.1016/S0926-860X(99)00497-4.

[36] T. Montanari, M. Bevilacqua, G. Busca, Use of nitriles as probe molecules for the accessibility of the active sites and the detection of complex interactions in zeolites through IR spectroscopy, Appl. Catal. A Gen. 307 (2006) 21–29. doi:10.1016/j.apcata.2006.03.003.

[37] M. Hunger, Catalytically Active Sites: Generation and Characterization, in: J. Čejka, A. Corma, S. Zones (Eds.), Zeolites Catal. Synth. React. Appl., Wiley-

VCH Verlag GmbH & Co. KGaA, Weinheim, 2010: pp. 493–546. doi:10.1002/9783527630295.ch17.

[38] S.A. Channiwala, P.P. Parikh, A unified correlation for estimating HHV of solid , liquid and gaseous fuels, Fuel. 81 (2002) 1051–1063.

[39] A.F. Costa, H.S. Cerqueira, J.M.M. Ferreira, N.M.S. Ruiz, S.M.C. Menezes, BEA and MOR as additives for light olefins production, Appl. Catal. A Gen. 319 (2007) 137–143. doi:10.1016/j.apcata.2006.11.027.

[40] S. Gutiérrez-Rubio, A. Berenguer, J. Přech, M. Opanasenko, C. Ochoa-Hernández, P. Pizarro, J. Čejka, D.P. Serrano, J.M. Coronado, I. Moreno, Guaiacol hydrodeoxygenation over Ni2P supported on 2D-zeolites, Catal. Today. 345 (2020) 48–58. doi:10.1016/j.cattod.2019.11.015.

[41] J.C. Groen, L.A.A. Peffer, J.A. Moulijn, J. Pérez-Ramírez, Mechanism of hierarchical porosity development in MFI zeolites by desilication: The role of aluminium as a pore-directing agent, Chem. - A Eur. J. 11 (2005) 4983–4994. doi:10.1002/chem.200500045.

[42] F.Z. Benabid, N. Kharchi, F. Zouai, A.H.I. Mourad, D. Benachour, Impact of co-mixing technique and surface modification of ZnO nanoparticles using stearic acid on their dispersion into HDPE to produce HDPE/ZnO nanocomposites, Polym. Polym. Compos. 27 (2019) 389–399. doi:10.1177/0967391119847353.

[43] B. Papajanı, E. Vataj, A. V. Hasımı, A. Sinanaj, The study of the influence of additives in the crystallinity of recycled LDPE by IR and XRD analysis, RAD Conf. Proc. 3 (2019) 236–240. doi:10.21175/RadProc.2018.49.

[44] G. Yuan, D. Chen, L. Yin, Z. Wang, L. Zhao, J.Y. Wang, High efficiency chlorine removal from polyvinyl chloride (PVC) pyrolysis with a gas-liquid fluidized bed reactor, Waste Manag. 34 (2014) 1045–1050. doi:10.1016/j.wasman.2013.08.021.

[45] H. Bockhorn, A. Hornung, U. Hornung, P. Jakobströer, M. Kraus, Dehydrochlorination of plastic mixtures, J. Anal. Appl. Pyrolysis. 49 (1999) 97–106. doi:10.1016/S0165-2370(98)00124-7.

[46] S. Ma, J. Lu, J. Gao, Study of the low temperature pyrolysis of PVC, Energy and Fuels. 16 (2002) 338–342. doi:10.1021/ef0101053.

[47] I.C. McNeill, L. Memetea, W.J. Cole, A study of the products of PVC thermal degradation, Polym. Degrad. Stab. 49 (1995) 181–191. doi:10.1016/0141-3910(95)00064-S.

[48] A. Torikai, H. Hasegawa, Accelerated photodegradation of poly(vinyl chloride), Polym. Degrad. Stab. 63 (1999) 441–445. doi:10.1016/S0141-3910(98)00125-6.

[49] J.L. Gardette, S. Gaumet, J. Lemaire, Photooxidation of Poly (vinyl chloride). 1. A Reexamination of the Mechanism, Macromolecules. 22 (1989) 2576–2581. doi:10.1021/ma00196a005.

[50] J. Pan, H. Jiang, T. Qing, J. Zhang, K. Tian, Transformation and kinetics of chlorine-containing products during pyrolysis of plastic wastes, Chemosphere. 284 (2021) 131348. doi:10.1016/j.chemosphere.2021.131348.

[51] W. Bi, T. Chen, R. Zhao, Z. Wang, J. Wu, J. Wu, Characteristics of a CaSO4 oxygen carrier for chemical-looping combustion:Reaction with polyvinylchloride pyrolysis gases in a two-stage reactor, RSC Adv. 5 (2015) 34913–34920. doi:10.1039/c5ra02044a.

[52] S.S. Suresh, S. Mohanty, S.K. Nayak, Composition analysis and characterization of waste polyvinyl chloride (PVC) recovered from data cables, Waste Manag. 60 (2017) 100–111. doi:10.1016/j.wasman.2016.08.033.

[53] J. Yang, R. Miranda, C. Roy, Using the DTG curve fitting method to determine the apparent kinetic parameters of thermal decomposition of polymers, Polym. Degrad. Stab. 73 (2001) 455–461. doi:10.1016/S0141-3910(01)00129-X.

[54] M.R. Jung, F.D. Horgen, S. V. Orski, V. Rodriguez C., K.L. Beers, G.H. Balazs, T.T. Jones, T.M. Work, K.C. Brignac, S.J. Royer, K.D. Hyrenbach, B.A. Jensen, J.M. Lynch, Validation of ATR FT-IR to identify polymers of plastic marine debris, including those ingested by marine organisms, Mar. Pollut. Bull. 127 (2018) 704–716. doi:10.1016/j.marpolbul.2017.12.061.

[55] Y. Zhang, Y. Xu, Y. Song, Q. Zheng, Study of poly(vinyl chloride)/acrylonitrile-styrene-acrylate blends for compatibility, toughness, thermal stability and UV irradiation resistance, J. Appl. Polym. Sci. 130 (2013) 2143–2151. doi:10.1002/app.39405.

[56] M. Beltran, A. Marcilla, Fourier transform infrared spectroscopy applied to the

study of PVC decomposition, Eur. Polym. J. 33 (1997) 1135–1142. doi:10.2174/2213235x05666170502104238.

[57] A. Ul-Hamid, K.Y. Soufi, L.M. Al-Hadhrami, A.M. Shemsi, Failure investigation of an underground low voltage XLPE insulated cable, Anti-Corrosion Methods Mater. 62 (2015) 281–287. doi:10.1108/ACMM-02-2014-1352.

[58] D.P. Serrano, J. Aguado, J.M. Escola, Catalytic cracking of a polyolefin mixture over different acid solid catalysts, Ind. Eng. Chem. Res. 39 (2000) 1177–1184. doi:10.1021/ie9906363.

[59] V.P.S. Caldeira, A. Peral, M. Linares, A.S. Araujo, R.A. Garcia-Muñoz, D.P. Serrano, Properties of hierarchical Beta zeolites prepared from protozeolitic nanounits for the catalytic cracking of high density polyethylene, Appl. Catal. A Gen. 531 (2017) 187–196. doi:10.1016/j.apcata.2016.11.003.